



# Air segmented amplitude modulated multiplexed flow analysis with software-based phase recognition: Determination of phosphate ion



Takeshi Ogusu<sup>a</sup>, Katsuya Uchimoto<sup>b</sup>, Masaki Takeuchi<sup>c</sup>, Hideji Tanaka<sup>c,\*</sup>

<sup>a</sup> Graduate School of Pharmaceutical Sciences, Tokushima University, Shomachi 1-78-1, Tokushima 770-8505, Japan

<sup>b</sup> Faculty of Pharmaceutical Sciences, Tokushima University, Shomachi 1-78-1, Tokushima 770-8505, Japan

<sup>c</sup> Institute of Health Biosciences, Tokushima University, Shomachi 1-78-1, Tokushima 770-8505, Japan

## ARTICLE INFO

### Article history:

Received 27 June 2013

Received in revised form

1 October 2013

Accepted 1 October 2013

Available online 10 October 2013

### Keywords:

Air segmentation

Amplitude modulation

Flow analysis

Fast Fourier transform

Determination of phosphate ion

Malachite Green method

## ABSTRACT

Amplitude modulated multiplexed flow analysis (AMMFA) has been improved by introducing air segmentation and software-based phase recognition. Sample solutions, the flow rates of which are respectively varied at different frequencies, are merged. Air is introduced to the merged liquid stream in order to limit the dispersion of analytes within each liquid segment separated by air bubbles. The stream is led to a detector with no physical deaeration. Air signals are distinguished from liquid signals through the analysis of detector output signals, and are suppressed down to the level of liquid signals. Resulting signals are smoothed based on moving average computation. Thus processed signals are analyzed by fast Fourier transform. The analytes in the samples are respectively determined from the amplitudes of the corresponding wave components obtained. The developed system has been applied to the simultaneous determinations of phosphate ions in water samples by a Malachite Green method. The linearity of the analytical curve ( $0.0\text{--}31.0 \mu\text{mol dm}^{-3}$ ) is good ( $r^2 > 0.999$ ) and the detection limit ( $3.3\sigma$ ) at the modulation period of 30 s is  $0.52 \mu\text{mol dm}^{-3}$ . Good recoveries around 100% have been obtained for phosphate ions spiked into real water samples.

© 2013 Elsevier B.V. All rights reserved.

## 1. Introduction

Amplitude modulated multiplexed flow analysis (AMMFA) is a new concept of continuous flow analysis [1]. Pieces of information on sample solutions are amplitude modulated by varying their flow rates at different frequencies, and are multiplexed by merging the solutions. The pieces can be derived from a single continuous analytical signal, obtained downstream, through a frequency analysis such as fast Fourier transform (FFT) [1–4] and lock-in detection [5]. As for such application of FFT to flow analyses, Szostek and Trojanowicz [6] reported a flow injection analysis of nitrite by biamprometry, where signal-to-noise ratio and throughput rate for repeated injections were greatly improved by FFT of detector output signals. López-García et al. [7] reported a more relevant concept to the present study. Two copper solutions were simultaneously supplied to the nebulizer of a flame atomic absorption spectrophotometer at modulated flow rates. The ratio of amplitudes of interest, obtained by Fourier transform of analytical signals, was proportional to that of copper concentrations in two solutions. Thus, the analyte concentration in one solution can be determined if that in the other solution is known.

We have applied AMMFA to the simultaneous analysis of multiple samples, where analytes were food dyes [1], ferrous ion [1] and chloride ion [2]. However, amplitude damping caused by axial dispersion of sample solutions in the conduit resulted in the decrease in sensitivity of the measurement. In the previous paper [3], we introduced an air segmentation concept, which had been originated by Skeggs [8,9] in the 1950s and applied later to continuous flow analysis [10–12], monosegmented continuous flow method (segmental flow injection analysis) [13–17] and so on, to AMMFA in order to limit the axial dispersion. The air segmented AMMFA was applied to the determination of phosphate ions or nitrite ions. The effect of air segmentation on the limitation of the dispersion was more pronounced at shorter modulation period and longer flow path length. The sensitivity was increased maximally by a factor of 2.7 compared with that obtained by an AMMFA with no air segmentation. However, the air bubbles needed to be removed just before the detection through a porous membrane, because they would cause severe noises against FFT analysis of liquid signals. Considerable amplitude damping through the dispersion still occurred after the phase separation.

In the present paper, we report air segmented AMMFA with no physical deaeration. Air bubbles are not removed but directly delivered to the flow cell of a UV/vis detector together with liquid stream in order to prevent the dispersion and to preserve high amplitude. Instead, air signals are suppressed down to the level of

\* Corresponding author. Tel.: +81 88 633 7285; fax: +81 88 633 9057.  
E-mail address: [h.tanaka@tokushima-u.ac.jp](mailto:h.tanaka@tokushima-u.ac.jp) (H. Tanaka).

liquid signals and smoothed with an in-house program. Thus processed signals are analyzed by FFT for the simultaneous determination of analytes in multiple samples. First, software parameters are optimized using Methyl Orange as an analyte, because no consideration on the coloration is necessary. The validity of the present concept is then evaluated by applying to the determination of phosphate ions, because phosphorus has been paid much attention recently with respect to the depletion of phosphorus resources [18], in addition to eutrophication. A malachite Green method [19,20] is selected due to its inherent high sensitivity. The proposed concept of air segmented AMMFA with no physical deaeration makes it possible to perform simultaneous determination of phosphate ions at  $\mu\text{mol dm}^{-3}$  level in multiple samples. The method has been applied to the determination of phosphate ions in river, pond, canal and moat water samples.

## 2. Experimental

### 2.1. Flow system

Fig. 1 shows the flow system configured in the present study. The system was of five channels manifold. Teflon tubing (0.5 mm i.d.) was used as conduit unless otherwise stated. Four peristaltic pumps ( $P_1$ ,  $P_2$ ,  $P_3$  and  $P_4$ ; Rainin Dynamax RP-1, USA) were used for delivering solutions, and one pump ( $P_5$ ; the same model as  $P_1$ – $P_4$ ) was for air. Pharmed tubing with 0.51 mm i.d. was used for  $P_1$ – $P_3$  and  $P_5$  as pump tubes and the tubing with 0.79 mm i.d. was used for  $P_4$ . The flow rates of sample solutions  $S_1$  and  $S_2$  delivered using  $P_1$  and  $P_2$  were varied in the range from 0 to  $0.25 \text{ cm}^3 \text{ min}^{-1}$ , but at different periods (typically, 30 and 20 s, respectively). The flow rates were controlled by sinusoidal controller output voltages ( $V_{c1}$  and  $V_{c2}$ , respectively) generated from a signal generator (SG; NF Corp. WF1974, Japan). The flow rate of color-forming reagent solution R delivered using  $P_3$  was kept constant at  $0.6 \text{ cm}^3 \text{ min}^{-1}$ . Both sample solutions and reagent solution were merged at a confluence point (polypropylene joint) while the total flow rate was held constant at  $1.2 \text{ cm}^3 \text{ min}^{-1}$  by  $P_4$ . The  $P_4$  is positioned upstream of an air-inflow joint (described below) for reliable liquid delivering and for easy comparison between air segmented AMMFA (present method) and non-segmented AMMFA (previous method [1]). The reason for the constant total flow rate is to keep the lag time between the merging the solutions upstream and the sensing the merged solution downstream. Water is, therefore, aspirated to the confluence point for compensating the difference of the total flow rate ( $1.2 \text{ cm}^3 \text{ min}^{-1}$ ) and the sum of the flow rates of the sample solutions and the reagent solution ( $0.6$ – $1.1 \text{ cm}^3 \text{ min}^{-1}$ ). Air bubbles were introduced from the fifth channel at a constant flow rate of  $0.13 \text{ cm}^3 \text{ min}^{-1}$ . The peristaltic pump

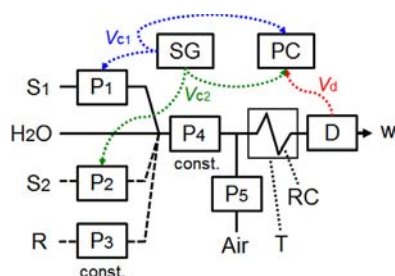


**Fig. 1.** Schematic diagram of flow system. A two-channel system (solid line) was used for the determination of Methyl Orange. A four-channel system (solid and broken lines) was used for the determination of phosphate ion. S, Sample solution; R, reagent solution;  $\text{H}_2\text{O}$ , water; w, waste;  $P_1$ – $P_5$ , peristaltic pumps; RC, reaction coil; D, spectrophotometer; SG, signal generator; PC, laptop computer with a card type A/D–D/A converter;  $V_{c1}$  and  $V_{c2}$ , controller output voltages;  $V_d$ , detector output voltage.

( $P_5$ ) and T-shaped polypropylene joint (AS ONE, VFT 106, Japan) was used for the air introduction, because this combination had been found to give sufficiently allowable precision (RSD of air-bubble volume:  $< 5\%$  [3]). The merged solution segmented by the air bubbles was led to a reaction coil (RC; 0.5 mm i.d. and 0.5 m long) in order to accelerate color reaction at elevated temperature ( $50^\circ\text{C}$ ). The temperature of RC was controlled with a temperature sensor (TOP L-TN-4-PT100, Japan), a silicon rubber heater (TOP 5099-01,  $100 \times 25 \text{ mm}$ , Japan) and a temperature controller (Toho BX-303, Japan). Thus reacted solution was introduced to a hand-made flow cell (quartz tubing), which was set in a spectrophotometer (D; Shimadzu SPD-10Avp or SPD-10AVvp, Japan; time constant: 0.05 s) for absorbance measurement. Analytical wavelength was 600 nm, unless otherwise stated. The incident beam is introduced not axially but perpendicularly to the cell (optical path length: 1 mm) in order to differentiate between liquid and air segments at the expense of sensitivity. The detector output voltage  $V_d$  as well as  $V_{c1}$  and  $V_{c2}$  were quantized by an A/D–D/A converter (Measurement Computing PC-CARD-DAS16/12-AO, USA). Resulting digital data were acquired in a laptop computer (PC; Toshiba DynaBook Satellite 1850 SA120C/4, Japan) as a Microsoft Excel format. An in-house program written in Visual Basic was used to acquire data, analyze them and graphically display the results automatically. Software-based phase recognition and FFT analysis will be described in Section 2.3.

### 2.2. Reagents and samples

Various methods such as spectrophotometry, fluorometry, chemiluminescence analysis, inductively coupled plasma atomic emission spectrometry, potentiometry, voltammetry and amperometry have been developed for the determination of phosphate ion, as reviewed by Worsfold et al. [21], Estela and Cerdà [22], Motomizu and Li [23], and Mesquita et al. [24]. In the present system with the UV/vis detector, a Malachite Green spectrophotometry [19,20] is adopted because it is inherently more sensitive than the most commonly employed Molybdenum Blue spectrophotometry by a factor of one magnitude. The color-forming reagent comprised  $1.6 \times 10^{-2} \text{ mol dm}^{-3}$  ammonium molybdate,  $4.0 \times 10^{-3} \text{ mol dm}^{-3}$  Malachite Green and  $1.3 \text{ mol dm}^{-3}$  sulfuric acid. Polyvinyl alcohol of 2000 average polymerization degree (0.5% as final concentration) was added to the reagent solution as a stabilizer for the ion-pair of Malachite Green and phosphomolybdate ion, according to the recommendation by Motomizu et al. [19].

All the reagents used were of analytical reagent grade purchased from Kanto Chemicals (Tokyo, Japan), Nacalai Tesque (Kyoto, Japan) or Wako Chemical Industries (Osaka, Japan). The reagents were used without further purification. Zartorius Arrium 611 DI grade deionized water was used throughout.

Real water samples were collected from the Fukuroi Irrigation Canal, the moat of Shozui Castle, the Iio River and the Naka Pond in urban area in Tokushima Prefecture, Japan. The samples were each filtered through a disposable disk filter with a pore size of  $0.45 \mu\text{m}$  (Kanto Chemical Co. 96904-00, Tokyo, Japan). Chloroform (0.5 vol% as final concentration) was added to the respective filtrates as a preservative [25], and thus prepared samples were stored in clean polypropylene bottles in a refrigerator at  $4^\circ\text{C}$ .

### 2.3. Data processing

Commercial Instrument “AutoAnalyzer”, which had been developed by Tecnicon Corporation based on the invention by Skeggs [8,9], has adopted software-based air recognition since early stages of commercialization. Independently, Habig et al. [26] reported “bubble gating”, a signal-processing based deaeration technique,

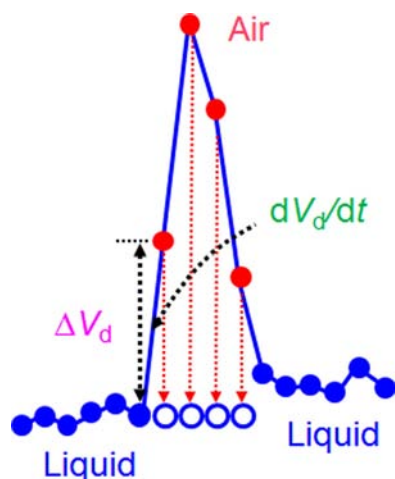


**Fig. 2.** Scheme of software-based deaeration.  $dV_d/dt$ , the slope of  $V_d$ ;  $\Delta V_d$ , the deviation of  $V_d$  from the latest liquid signal.

**Table 1**  
Typical values of main software parameters.

Principal software parameters		Typical values
Controller output signal $V_{c1}$	Amplitude/ $V_{p-p}$	0–5
	Period/s	30
Controller output signal $V_{c2}$	Amplitude/ $V_{p-p}$	0–5
	Period/s	20
Thresholds for air recognition	Slope of $V_d/V \text{ s}^{-1}$	0.45
	Deviation of $V_d$ from the latest liquid $V_d/V$	0.35
Number of data for moving average		31
Number of data for FFT computation		8
Sampling frequency/Hz		8.53333 (5)
Interval of FFT computation/s		1.875 (2)

The values in the parentheses are original values imputed by an operator. These values are automatically changed to the values so that they become compatible with FFT algorithm.

where the gate was activated by the change in conductance. Electronic bubble gate [27,28], refractive index based bubble gate [29] and digital bubble gate [30] have also been reported. Liu and Dasgupta reported a dual-wavelength spectrometry [31] and a conductometry [32] for aqueous/organic phase recognition in flow injection extraction systems. In the present study, air signals are recognized based on the shape of the signals, as schematically shown in Fig. 2. Air gives much higher detector output signals than those by liquid. The  $V_d$  corresponding to air showed, therefore, steep upward peaks. In order to recognize such air signals, we defined two kinds of threshold values: one is for the  $V_d$  slope ( $dV_d/dt$ ) and the other for the  $V_d$  deviation from the latest liquid signal ( $\Delta V_d$ ). If acquired  $V_d$  exceeds either of the threshold values, it is regarded as air signal. In this case, the latest liquid  $V_d$  value (open circles) is held instead of the acquired  $V_d$  (closed circles). The resulting track of  $V_d$  is of stair-like nature. The  $V_d$  is, therefore, further processed by moving average smoothing technique.

The principle of FFT for AMMFA was described in detail elsewhere [1]. Briefly, the analytical signal  $V_d$  contains amplitude modulated and multiplexed pieces of information on  $S_1$  and  $S_2$ . The  $V_d$  is of periodic nature, so long as the concentrations of analytes in the samples are invariant. The period of  $V_d$  corresponds to the least common multiple of the periods of  $V_{c1}$  and  $V_{c2}$ . This  $V_d$  period is used as the length of the window for FFT analysis. Typical software parameters are listed in Table 1. The periods of  $V_{c1}$  and  $V_{c2}$  are 30 s and 20 s, respectively; thus that of  $V_d$  is 60 s. The  $V_d$  data are acquired at the sampling frequency of 8.533 Hz. Thus, 512

data are obtained in the period of 60 s. Eight ( $=2^3$ ) data,  $x_n$ , in this period (i.e., every 16 points) are used for FFT computation as expressed below

$$X_k = \frac{1}{N} \sum_{n=0}^{N-1} x_n \exp\left(-j \frac{2\pi nk}{N}\right), \quad N = 8 \quad (1)$$

where  $N$  is the number of the data for FFT analysis and  $j$  is the imaginary number. The temporal profile of the amplitudes can be obtained in real time by moving the window for FFT analysis. FFT computation is carried out every 1.875 s by using new 8 data set.

### 3. Result and discussion

#### 3.1. Optimization of software-based phase recognition

Two kinds of threshold values for the software-based phase recognition were optimized using an aqueous solution of Methyl Orange as a sample solution. For this purpose,  $S_2$  and R channels shown in Fig. 1 were closed. Sample solution was introduced from  $S_1$  channel alone. Analytical wavelength was 470 nm. Fig. 3A shows typical raw signals for a  $15 \text{ mg dm}^{-3}$  ( $=45.8 \mu\text{mol dm}^{-3}$ ) Methyl Orange solution, where the period for modulation is 30 s.

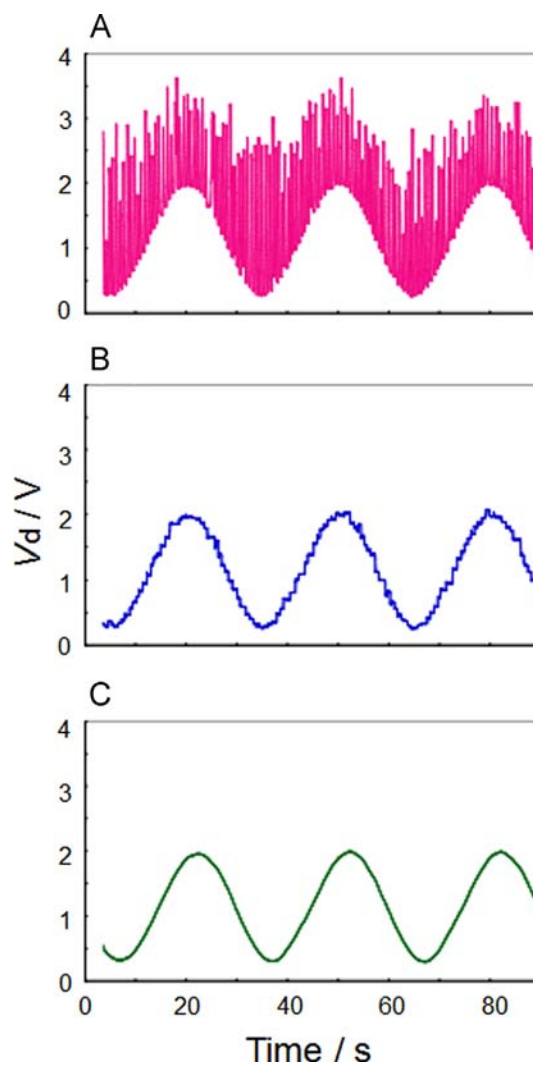


**Fig. 3.** Flow signals of amplitude modulated flow analysis. (A) Raw analytical signals. (B) Signals after automatic software-based deaeration. (C) Signals after automatic software-based deaeration and subsequent moving average smoothing. Sample, aqueous solution of Methyl Orange ( $15 \text{ mg dm}^{-3}$ ).  $V_c$  period, 30 s.

Sharp upward peaks correspond to the signals for air segments. In order to recognize such air signals by our software, we carefully analyzed the data and determined the two kinds of the threshold values after some trials and errors. In this case, the employed values were  $1.0 \text{ V s}^{-1}$  for the absolute value of  $V_d$  slope, and  $0.7 \text{ V}$  for the  $V_d$  deviation from the latest liquid signal. Fig. 3B shows the analytical signals for the same samples after the automatic air signal processing using the above mentioned threshold values. It shows our software could completely remove air signals.

Further, thus obtained stair-like signals were smoothed by moving average computation. The number of data points for the computation was examined. Data sets of 11, 21, 31, 41, 51, 71 and 101 points were used for the computation and the results were compared with those before the processing. The RSD of the amplitude of the fundamental wave component (period: 30 s),  $A_{1st}$ , after the smoothing improved with the number of data points and became almost constant when the number was higher than 31 (see Supplementary material, Fig. S1). That is, the RSD values ( $n=24$ ) were 3.1%, 1.9%, 1.1%, 0.9%, 1.3%, 1.2%, 0.6% and 0.9% for the number of data points of 1 (no smoothing), 11, 21, 31, 41, 51, 71 and 101, respectively. However, when the number became higher than 31,  $A_1$  decreased because of over-smoothing. That is, the values of  $A_{1st}$  were 0.774, 0.808, 0.807, 0.808, 0.782, 0.752, 0.710 and 0.638 V at the number of 1 (no smoothing), 11, 21, 31, 41, 51, 71 and 101, respectively. Data set of 31 points (in the span of 3.63 s at the sampling frequency of 8.533 Hz) was, therefore, used for moving average computation. Fig. 3C shows the analytical signals thus smoothed. Smooth signals that preserve high amplitude were obtained by the present automatic software-based deaeration and subsequent moving average processing.

Analytical curves were constructed from five standard solutions sets of Methyl Orange ( $0\text{--}15 \text{ mg dm}^{-3}$ ). The flow rates of  $P_1$  and  $P_4$  were  $0\text{--}0.9$  (modulated at the period of 30 s) and  $1.0$  (constant)  $\text{cm}^3 \text{ min}^{-1}$ , respectively. The  $P_5$  channel was open for the air segmented AMMFA (flow rate:  $0.18 \text{ cm}^3 \text{ min}^{-1}$ ) or closed for non-segmented AMMFA. Linear regression lines obtained by air segmented AMMFA with no deaeration (present method), by air segmented AMMFA with deaeration (previous method [3]) and by non-segmented AMMFA (previous method [1]) are  $A_{1st}=0.058 C_{MO}+0.001$  ( $r^2=0.9999$ ),  $A_{1st}=0.039 C_{MO}+0.002$  ( $r^2=0.9998$ ) and  $A_{1st}=0.033 C_{MO}+0.005$  ( $r^2=0.9990$ ), respectively, where  $C_{MO}$  means the concentration of Methyl Orange in  $\text{mg dm}^{-3}$ . Respective LOD ( $3.3\sigma$ ) were 0.348, 0.406 and  $0.885 \text{ mg dm}^{-3}$ . These results suggest the introductions of air segmentation and software-based deaeration techniques are effective for the improvements in the sensitivity and LOD of AMMFA.

### 3.2. Simultaneous analysis of two samples

The developed system was applied to the simultaneous determination of phosphate ions in two samples. Analytical curves were constructed from five standard solutions. The concentration of phosphate ions in  $S_1$  was changed stepwise from 0 through 7.75,

15.50, 23.25 to  $31.00 \text{ } \mu\text{mol dm}^{-3}$  and that in  $S_2$  was done so in the reverse order for  $S_1$ . The periods of  $V_{c1}$  and  $V_{c2}$  were set at 30 and 20 s, respectively, because shorter control periods would cause considerable amplitude damping [3]. In this case, 60 s is the length of FFT window. The amplitudes of the second and the third harmonic wave components in  $V_d$ , therefore, correspond to the concentrations of phosphate ions in  $S_1$  and  $S_2$ , respectively. The threshold values for the  $V_d$  slope and the  $V_d$  deviation were  $0.45 \text{ V s}^{-1}$  and  $0.35 \text{ V}$ , respectively, as listed in Table 1. The results are summarized in Table 2 and shown in Fig. S2 in Supplementary material together with those obtained by non-segmented AMMFA obtained in the present study using the previous method [1]. The linearity of the obtained analytical curves was good ( $r^2 > 0.999$ ). The sensitivity was increased by a factor of 1.46 and 1.66 for  $S_1$  and  $S_2$ , respectively. Lower LOD values ( $0.52$  and  $0.75 \text{ } \mu\text{mol dm}^{-3}$  ( $=16.1$  and  $23.2 \text{ } \mu\text{g dm}^{-3}$  as P) at  $3.3\sigma$  for  $S_1$  and  $S_2$ , respectively) were obtained by the proposed approach compared with those ( $2.35$  and  $4.97 \text{ } \mu\text{mol dm}^{-3}$ ) by the non-segmented AMMFA. The difference of the slopes between  $S_1$  and  $S_2$  are attributed to the difference in the control period. That is, amplitude damping is more pronounced when the control period becomes shorter as discussed in the previous papers [2,3], resulting in lower slope for  $S_2$  (the period: 20 s) than that for  $S_1$  (the period: 30 s). The benefit of air segmentation is greater at shorter control period, as discussed before [3]. Analytical data are obtained every 1.875 s, corresponding to the  $0.01875 \text{ cm}^3$  of reagent consumption per determination. The precisions of 60 successive determinations of  $31.0 \text{ } \mu\text{mol dm}^{-3}$  phosphate ion were 2.35% and 4.59% for  $S_1$  and  $S_2$ , respectively. As for the influence of coexisting ions on the Malachite Green method coupled with an amplitude modulated approach was reported in the previous paper [5]; tolerable limits of the ions tested were comparable to those reported in literatures [18,33].

### 3.3. Analyses of real water samples

The present method was applied to the determination of phosphate ions in real water samples. In order to evaluate the applicability of the present system to continuous monitoring, the real water samples of the Fukuroi Irrigation Canal, the moat of Shozui Castle, the Iio River, the Naka Pond and again the Fukuroi Irrigation Canal were successively introduced from  $S_1$  channel, each duration time being 5 min. Replacement of the solutions was carried out manually. On the other hand, the Fukuroi Irrigation Canal water was delivered from  $S_2$  throughout. The periods of  $V_{c1}$  and  $V_{c2}$  were 30 and 20 s, respectively. Figs. 4 and 5 show  $V_d$  and amplitudes obtained, respectively. The amplitudes of the second and the third harmonic wave components ( $A_{2nd}$  and  $A_{3rd}$ ) correspond to the concentrations of phosphate ions in  $S_1$  and  $S_2$ , respectively. The amplitudes of the fundamental and the fourth harmonic wave components ( $A_{1st}$  and  $A_{4th}$ , respectively) should ideally be zero because no control signals with the periods of 60 s and 15 s were employed in this experiment. The magnitude of the

**Table 2**  
Analytical curves for the simultaneous determination of phosphate ions in two samples.

Sample	Air segmented AMMFA with no deaeration (proposed method)				Non-segmented AMMFA			
	Slope	Intercept	$r^2$	LOD/ $\mu\text{mol dm}^{-3}$	Slope	Intercept	$r^2$	LOD/ $\mu\text{mol dm}^{-3}$
$S_1$	0.0041	0.0061	0.9999	0.52	0.0028	0.0042	0.9984	2.35
$S_2$	0.0033	0.0040	0.9998	0.75	0.0020	0.0040	0.9930	4.97

The flow rates of  $S_1$  and  $S_2$  were varied with the periods of 30 and 20 s, respectively. Analytical curves are expressed as  $A = \text{slope} \times C + \text{intercept}$ , where  $A$  is the amplitude of the second (for  $S_1$ ) and the third (for  $S_2$ ) harmonic wave component;  $C$  is the concentration of phosphate ion in  $\mu\text{mol dm}^{-3}$ .

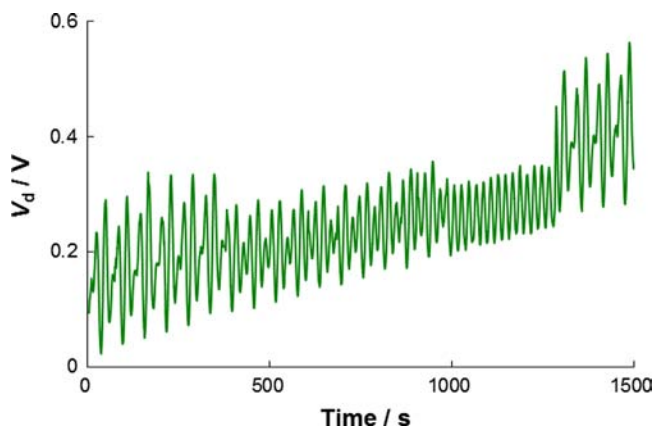


**Fig. 4.** Analytical signals  $V_d$  for continuous measurement of phosphate ions in two real water samples. Analytical wavelength was 625 nm. The periods of  $V_{c1}$  and  $V_{c2}$  are 30 and 20 s, respectively. The ordinate scale is enlarged by a factor of 6.67 compared with Fig. 3 in order to emphasize the drift.

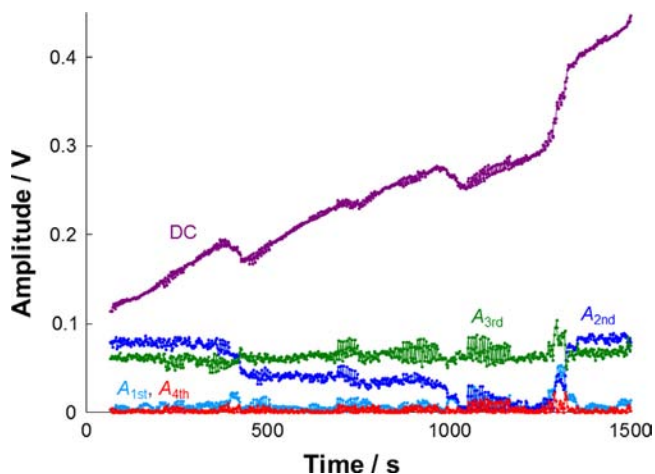


**Fig. 5.** Amplitudes of wave components of  $V_d$ . DC, direct current component.  $A_{1st}$ – $A_{4th}$ , amplitudes of the fundamental, second harmonic, third harmonic and fourth harmonic wave components, respectively. The periods of control signals for sample flow rates were 30 s and 20 s for  $S_1$  and  $S_2$ , respectively. The amplitudes of the second and the third harmonic wave components correspond to the concentrations of phosphate ions in  $S_1$  and  $S_2$ , respectively.

direct current (DC) corresponds to the average absorbance in the FFT window and varies depending on the concentration of phosphate ions in the two samples. Figs. 4 and 5 show that both  $V_d$  and DC drifted upwards in the course of the measurement. This drift is attributed to the adsorption of the green ion-pair formed from Malachite Green and phosphomolybdate ion on the optical window of the flow cell [33], even though polyvinyl alcohol was added in the color-forming reagent as a stabilizer. Nevertheless, almost constant values were obtained for  $A_{3rd}$ , as shown in Fig. 5. These results show that the present method, where the determination is based not on the value of absorbance itself but on the amplitude of the absorbance, is unsusceptible to the baseline drift, as in the previous study with lock-in detection [5]. Deal and Easley reported the combination of drop-based chopper and lock-in detection in microfluidic absorption measurement having drift trend [34]. Similar measurements were carried out for the sets of standard solution (0–15.5  $\mu\text{mol dm}^{-3}$ ) in order to construct analytical curves. The concentrations of phosphate ions in the real water samples were determined using the analytical curve thus obtained. Analytical values obtained from  $A_{2nd}$  in Fig. 5 were  $8.26 \pm 0.33$  ( $n=128$ ; time=80.51–318.63 s),  $4.25 \pm 0.33$  ( $n=128$ ;

**Table 3**  
Determination of phosphate ion in real water samples (Tokushima, Japan).

Sample		$C_{\text{Pi,Add}}/\mu\text{mol dm}^{-3}$		$C_{\text{Pi,Fnd}}/\mu\text{mol dm}^{-3}$		Recovery, %	
$S_1$	$S_2$	$S_1$	$S_2$	$S_1$	$S_2$	$S_1$	$S_2$
A	B	0	0	$8.68 \pm 0.27$	$4.22 \pm 0.34$	–	–
				$8.43 \pm 0.25$	$4.37 \pm 0.40$	–	–
		10	0	$18.81 \pm 0.35$	$4.38 \pm 0.52$	101.3	–
				$18.41 \pm 0.68$	$4.13 \pm 0.85$	99.9	–
		0	10	$8.38 \pm 0.62$	$14.57 \pm 0.49$	–	103.5
		10	10	$8.91 \pm 0.49$	$14.47 \pm 0.74$	–	101.0
C	D	0	0	$18.42 \pm 0.86$	$14.67 \pm 0.82$	97.5	104.5
				$18.70 \pm 0.56$	$14.55 \pm 0.73$	102.7	101.7
		0	0	$3.53 \pm 0.36$	n.d.	–	–
				$3.49 \pm 0.29$	n.d.	–	–
		10	0	$13.74 \pm 0.52$	n.d.	102.1	–
				$13.84 \pm 0.49$	n.d.	103.5	–
	0	10	$3.68 \pm 0.34$	$10.46 \pm 0.35$	–	101.3	
			$3.59 \pm 0.37$	$10.53 \pm 0.37$	–	101.9	
	10	10	$13.87 \pm 0.75$	$10.49 \pm 1.04$	103.4	101.7	
			$13.73 \pm 0.33$	$10.53 \pm 0.43$	101.4	101.8	

Sampling from the Fukuroi Irrigation Canal (A); the moat of Shozui Castle (B); the Iio River (C); the Naka Pond (D). Sampling date: June 1, 2012. Phosphate ion was added as  $\text{NaH}_2\text{PO}_4$ . For each combination, the same measurements were carried out twice. Concentration of phosphate ion found is expressed as mean  $\pm$  s.d. ( $n=60$ ). The pH of the samples: 7.0 (A), 6.9 (B), 7.0 (C), 6.7 (D). The COD of the samples: 8.6 (A), 10.0 (B), 9.4 (C), 10.1, (D)  $\text{mg dm}^{-3}$ .

time=448.01–686.13 s) and  $3.58 \pm 0.40$  ( $n=128$ , time=748.01–986.13 s)  $\mu\text{mol dm}^{-3}$  for the Fukuroi Irrigation Canal, the moat of Shozui Castle and the Iio River, respectively. The same measurement was carried out once more. Analytical values for respective samples were  $8.46 \pm 0.42$ ,  $4.35 \pm 0.23$  and  $3.32 \pm 0.37$   $\mu\text{mol dm}^{-3}$ . As for the Naka Pond, the concentration was below the detection limit. These values are comparable to those obtained by a standard method [25] (Molybdenum Blue spectrophotometry with ascorbic acid reduction (batch method); analytical wavelength: 880 nm):  $8.273 \pm 0.056$  ( $n=3$ ),  $4.633 \pm 0.028$  ( $n=3$ ),  $3.484 \pm 0.028$  ( $n=3$ )  $\mu\text{mol dm}^{-3}$  and N.D., respectively.

Recovery tests were carried out by spiking a known amount of phosphate ions (0 or 10  $\mu\text{mol dm}^{-3}$  as final concentration) to each sample solution. The non-spiked and spiked sample solutions were analyzed by the proposed method. The results are listed in Table 3. Fig. S3 in Supplementary material shows an example of analytical signals,  $V_d$ , that give the data in the bottom row in Table 3. The pH and COD of the samples, the latter of which was determined according to an official method using permanganate in alkaline media [35], are shown in the footnote of the table as references. Good recoveries from 97.5% to 104.5% were obtained for the analytes spiked in the samples.

#### 4. Conclusion

Air segmented amplitude modulated multiplexed flow analysis has been improved by introducing software-based phase recognition. Air segmentation with software-based deaeration is effective for limiting axial dispersion, thus improving the sensitivity of AMMFA. Compared with the results obtained by the non-segmented AMMFA, the sensitivity of a Malachite Green method for phosphate determination is improved by a factor of 1.46–1.66, depending on the modulation period. The method has been applied to the determination of phosphate ion in real water samples. Although good recoveries around 100% are obtained for phosphate ions spiked into the samples, further improvement in sensitivity would be needed in order to apply the present method to less contaminated water samples. We are, therefore, studying

on AMMFA with online preconcentration and the results will be reported in future.

### Acknowledgments

The present study is partly supported by the Grant-in-Aid for Scientific Research (C) (21550083, 24550101) from the Japan Society for the Promotion of Science (JSPS).

### Appendix A. Supplementary materials

Supplementary materials associated with this article can be found in the online version at <http://dx.doi.org/10.1016/j.talanta.2013.10.001>.

### References

- [1] H. Tanaka, T. Mima, M. Takeuchi, H. Iida, *Talanta* 77 (2008) 576–580.
- [2] Y. Kurokawa, M. Takeuchi, H. Tanaka, *Anal. Sci.* 26 (2010) 791–796.
- [3] K. Inui, T. Uemura, T. Ogusu, M. Takeuchi, H. Tanaka, *Anal. Sci.* 27 (2011) 305–308.
- [4] H. Yoshida, K. Inui, M. Takeuchi, H. Tanaka, *Anal. Sci.* 28 (2012) 523–525.
- [5] T. Uemura, T. Ogusu, M. Takeuchi, H. Tanaka, *Anal. Sci.* 26 (2010) 797–801.
- [6] B. Szostek, M. Trojanowicz, *Chemom. Intell. Lab. Syst. J.* 22 (1994) 221–228.
- [7] I. López-García, M. Sánchez-Merlos, M. Hernández-Cordoba, *J. Anal. At. Spectrom.* 13 (1998) 1151–1154.
- [8] L.T. Skeggs, *Am. J. Clin. Pathol.* 28 (1957) 311–322.
- [9] L.T. Skeggs, *Anal. Chem.* 38 (1966) 31A–44A.
- [10] L. Snyder, J. Levine, R. Stoy, A. Conetta, *Anal. Chem.* 48 (1976) 942A–956A.
- [11] L.R. Snyder, H.J. Adler, *Anal. Chem.* 48 (1976) 1017–1022.
- [12] L.R. Snyder, H.J. Adler, *Anal. Chem.* 48 (1976) 1022–1027.
- [13] C. Pasquini, W.A. de Oliveira, *Anal. Chem.* 57 (1985) 2575–2579.
- [14] C. Pasquini, *Anal. Chem.* 58 (1986) 2346–2348.
- [15] L.C. Tian, X.P. Sun, Y.Y. Xu, Z.L. Zhi, *Anal. Chim. Acta* 238 (1990) 183–190.
- [16] Y. Hsieh, S.R. Crouch, *Anal. Chim. Acta* 303 (1995) 231–239.
- [17] Z.-L. Zhi, *Trends Anal. Chem.* 17 (1998) 411–417.
- [18] P.H. Abelson, *Science* 283 (1999) 2015.
- [19] S. Motomizu, T. Wakimoto, K. Toei, *Analyst* 108 (1983) 361–367.
- [20] S. Motomizu, T. Wakimoto, K. Toei, *Talanta* 30 (1983) 333–338.
- [21] P.J. Worsfold, L.J. Gimbert, U. Mankasingh, O.N. Omaka, G. Hanrahan, P.C.F. C. Gardolinski, P.M. Haygarth, B.L. Turner, M.J. Keith-Roach, I.D. McKelvie, *Talanta* 66 (2005) 273–293.
- [22] J.M. Estela, V. Cerdà, *Talanta* 66 (2005) 307–331.
- [23] S. Motomizu, Z.-H. Li, *Talanta* 66 (2005) 332–340.
- [24] R.B.R. Mesquita, M.T.S.O.B. Ferreira, I.V. Tóth, A.A. Bordalo, I.D. McKelvie, A.O.S. S. Rangel, *Anal. Chim. Acta* 701 (2011) 15–22.
- [25] JIS K 0101, *Kougyo-yosui Shiken Hoho* (Testing Methods for Industrial Water, in Japanese), 1998; JIS K 0102, *Kougyo-haisui Shiken Hoho* (Testing Methods for Industrial Wastewater, in Japanese), 2008, Japanese Industrial Standards Committee, Tokyo, Japan.
- [26] R.L. Habis, B.W. Schlein, L. Walters, R.E. Thiers, *Clin. Chem.* 15 (1969) 1045–1055.
- [27] W.E. Neeley, S. Wardlaw, M.E.T. Swinnen, *Clin. Chem.* 20 (1974) 78–80.
- [28] W.E. Neeley, S.C. Wardlaw, T. Yates, W.G. Hollingsworth, M.E.T. Swinnen, *Clin. Chem.* 22 (1976) 227–231.
- [29] W. Vogt, S.L. Braun, S. Wilhelm, H. Schwab, *Anal. Chem.* 54 (1982) 596–598.
- [30] C.J. Patton, M. Rabb, S.R. Crouch, *Anal. Chem.* 54 (1982) 1113–1118.
- [31] H. Liu, P.K. Dasgupta, *Anal. Chim. Acta* 288 (1994) 237–245.
- [32] H. Liu, P.K. Dasgupta, *Process Control Qual.* 7 (1995) 195–202.
- [33] A. Muñoz, F. Mas Torres, J.M. Estela, V. Cerdà, *Anal. Chim. Acta* 350 (1997) 21–29.
- [34] K.S. Deal, C.J. Easley, *Anal. Chem.* 84 (2012) 1510–1516.
- [35] Pharmaceutical Society of Japan (ed.), *Standard Methods of Analysis for Hygienic Chemist, with Commentary*, Kanehara Shuppan, Tokyo, 2010, pp. 875–877 (in Japanese).